NeuroImage: Clinical 2 (2013) 521–533

Contents lists available at ScienceDirect

NeuroImage: Clinical

journal homepage: www.elsevier.com/locate/ynicl

Assessing a standardised approach to measuring corticospinal integrity after stroke with DTI☆

Chang-hyun Park [a,*], Nancy Kou [a], Marie-Hélène Boudrias [a], E. Diane Playford [b,c], Nick S. Ward [a,b]

[a] Sobell Department of Motor Neuroscience and Movement Disorders, UCL Institute of Neurology, Queen Square, London WC1N 3BG, UK
[b] The National Hospital for Neurology and Neurosurgery, Queen Square, London WC1N 3BG, UK
[c] Department of Brain Repair and Rehabilitation, UCL Institute of Neurology, Queen Square, London WC1N 3BG, UK

ARTICLE INFO

Article history:
Received 27 December 2012
Received in revised form 4 April 2013
Accepted 4 April 2013
Available online 11 April 2013

Keywords:
Diffusion tensor imaging
Fractional anisotropy
Corticospinal tract
Stroke
Motor ability

ABSTRACT

The structural integrity of the corticospinal tract (CST) after stroke is closely linked to the degree of motor impairment. Simple and reliable methods of assessing white matter integrity within the CST would facilitate the use of this measure in routine clinical practice. Commonly, diffusion tensor imaging is used to measure voxel-wise fractional anisotropy (FA) in a variety of regions of interest (ROIs) representing the CST. Several methods are currently in use with no consensus about which approach is best. ROIs are usually either the whole CST or the posterior limb of the internal capsule (PLIC). These are created manually on brain images or with reference to an individual's CST determined by tractography. Once the ROI has been defined, the FA can be reported as an absolute measure from the ipsilesional side or as a ratio in comparison to the contralesional side. Both corticospinal tracking and manual ROI definition in individual stroke patients are time consuming and subject to bias. Here, we investigated whether using a CST template derived from healthy volunteers was a feasible method for defining the appropriate ROI within which to measure changes in FA. We reconstructed the CST connecting the primary motor cortex to the ipsilateral pons in 23 age-matched control subjects and 21 stroke patients. An average healthy CST template was created from the 23 control subjects. For each patient, FA values were then calculated for both the template CST and for their own CST. We compared patients' FA metrics between the two tracts by considering four measures (FA in the ipsilesional side, FA in the contralesional side, FA ratio of the ipsilesional side to the contralesional side and FA asymmetry between the two sides) and in two tract-based ROIs (whole tract and tract section traversing the PLIC). There were no significant differences in FA metrics for either method, except for contralesional FA. Furthermore, we found that FA metrics relating to CST damage all correlated with motor ability post-stroke equally well. These results suggest that the healthy CST template could be a surrogate structure for defining tract-based ROIs with which to measure stroke patients' FA metrics, avoiding the necessity for CST tracking in individual patients. CST template-based automated quantification of structural integrity would greatly facilitate implementation of practical clinical applications of diffusion tensor imaging.

1. Introduction

Diffusion tensor imaging (DTI) is commonly used to investigate tissue microstructure in the central nervous system, particularly through the measurement of fractional anisotropy (FA). FA reflects the degree of anisotropic diffusion (Basser and Pierpaoli, 1996) and is a potentially powerful tool for assessing residual structural architecture in a number of central nervous system disorders. After stroke for example, FA might be used to assess the integrity of the corticospinal tract (CST) to help predict motor outcomes or direct clinicians to the most appropriate therapy (Stinear et al., 2012). However, there are a variety of approaches used in assessing CST integrity with FA values; the lack of consensus over which is the most appropriate is a potential barrier to widespread clinical use of this tool.

FA values are often averaged across specific regions of interest (ROIs), for example the posterior limb of the internal capsule (PLIC). These ROIs can be defined with or without reference to the individual's CST reconstructed using tractography (Jayaram et al., 2012; Madhavan et al., 2011; Qiu et al., 2011; Stinear et al., 2007). In other words, tract-based ROIs are determined within the reconstructed CST of an individual subject and may refer to the whole tract (Lindenberg et al., 2012; Rüber et al., 2012) or a subsection of the tract (Globas et al., 2011; Lindenberg et al., 2010; Lotze et al., 2012; Puig et al., 2010,

* Corresponding author at: Sobell Department of Motor Neuroscience and Movement Disorders, UCL Institute of Neurology, 33 Queen Square, London WC1N 3BG, UK. Tel.: +44 20 3448 8776.
E-mail address: chang-hyun.park@ucl.ac.uk (C. Park).

2213-1582/$ – see front matter © 2013 The Authors. Published by Elsevier Inc. All rights reserved.
http://dx.doi.org/10.1016/j.nicl.2013.04.002

2011). Alternatively, anatomical landmark-based ROIs refer to regions manually delineated on the brain, relying on anatomical landmarks, without reconstruction of the CST by tractography (Jayaram et al., 2012; Lindberg et al., 2007; Liu et al., 2012; Madhavan et al., 2011; Qiu et al., 2011; Stinear et al., 2007; Yeo et al., 2011).

Once the ROI has been defined, the FA can be reported as an absolute measure from the ipsilesional side (FA_{ipsi}) (Jang et al., 2006; Lindenberg et al., 2012; Møller et al., 2007; Nelles et al., 2008; Pierpaoli et al., 2001; Puig et al., 2010) or contralesional side (FA_{contra}) (Jang et al., 2006; Lindenberg et al., 2012; Pierpaoli et al., 2001; Puig et al., 2010). Alternatively, the ratio of the ipsilesional to contralesional side (FA_{ratio}) (Globas et al., 2011; Jang et al., 2005; Lindberg et al., 2007; Lotze et al., 2012; Puig et al., 2010) or FA asymmetry ($FA_{asymmetry}$), defined as $(FA_{contra} - FA_{ipsi})/(FA_{contra} + FA_{ipsi})$ (Globas et al., 2011; Jayaram et al., 2012; Lindenberg et al., 2010; Madhavan et al., 2011; Qiu et al., 2011; Stinear et al., 2007) may be reported.

Many of these approaches have been used to demonstrate a relationship between tract integrity and motor ability in stroke patients, but the factors that will influence uptake of these approaches on a large scale include feasibility and reliability. Tract-based ROIs appear to be at least as reliable as approaches using anatomical landmark-based ROIs (Borich et al., 2012; Hong et al., 2008; Partridge et al., 2005; Tang et al., 2010). However, CST tracking in individual stroke patients is often difficult because of interruption of fibres by the infarct which can result in the unreliable morphology of the tracts. On the other hand, manual placement of ROIs in individual patients is also problematic being open to operator bias. In both cases the procedures are time consuming, limiting feasibility and therefore generalisability.

In this study, we have investigated how using a CST template acquired from healthy subjects performs in comparison to the approaches described above. Recently, tract templates acquired from healthy subjects have been used to quantify damage to thalamocortical connections in patients with traumatic brain injury (Squarcina et al., 2012) as well as CST integrity in stroke patients (Schulz et al., 2012). Here we systematically examine the effects of varying both the type of FA measurement (FA_{ipsi}, FA_{contra}, FA_{ratio} or $FA_{asymmetry}$) and spatial extent of an ROI (whole tract or tract section comprising the PLIC) when using CST acquired from either healthy subjects or from individual stroke patients. Since there is no gold standard in the assessment of CST integrity, our approach was to compare the relationship between CST integrity and motor ability in a group of chronic stroke patients. Based on our previous experience (Schulz et al., 2012), we hypothesised that CST integrity assessed using 'normal' and individual patient tracts would perform equally as well.

2. Methods

2.1. Subjects

Twenty-one stroke patients (53.90 ± 14.07 years) participated in this study. All had unilateral hemispheric infarcts occurring between 4 and 165 months previously. The clinical characteristics of the patients are described in Table 1. Twenty-three age-matched (p value = 0.4524) healthy subjects (50.61 ± 14.69 years) who reported no history of neurological illness, psychiatric history, vascular disease or hypertension served as controls.

Full written consent was obtained from each subject in accordance with the Declaration of Helsinki. The study was approved by the Joint Ethics Committee of the Institute of Neurology, UCL and National Hospital for Neurology and Neurosurgery, UCL Hospitals NHS Foundation Trust, London.

2.2. Motor tests

The patients showed motor deficits of the contralesional upper extremity which was assessed using the Action Research Arm Test (Lyle, 1981), grip strength (Sunderland et al., 1989) Motricity Index (Bohannon, 1999) and Nine-Hole Peg Test (Kellor et al., 1971). In order to alleviate floor and ceiling effects in individual scores, the first principle component (PC1) of the scores of the four motor tests was calculated as a representative measure of motor ability. PC1 accounted for 65.16% of the total variance of the four scores. Motor scores including the PC1 are listed in Table 1.

Table 1
Demographic and clinical characteristics of patients included in the study.

No	Age (years)	Time since stroke (months)	Gender	Affected hand	Lesion location	Lesion volume (mm^3)	Lesion load of CST (%)	Motor performance				
								ARAT (0-57)	GRIP (%)	MI -UL (0-100)	NHPT (%)	PC1 (a.u.)
1	77	26	F	R	NCM	1339.875	10.172	38	57.2	77.0	9.0	−0.1463
2	60	41	M	L	CM	44,931.375	0.087	39	20.1	65.0	0.0	−0.3016
3	59	79	M	L	CM	59,025.375	29.896	21	50.3	73.0	0.0	−0.2963
4	53	31	F	L	NCM	290.250	0.520	50	40.0	91.0	50.0	0.0414
5	51	60	M	R	NCM	1282.500	7.069	45	104.0	92.0	31.0	0.1194
6	66	26	M	R	CM	32,285.250	23.017	35	81.0	65.0	39.0	−0.0972
7	69	9	M	R	NCM	5943.375	0.000	57	80.5	100.0	69.7	0.2595
8	55	5	F	L	NCM	594.000	3.986	55	64.0	93.0	97.0	0.2405
9	61	13	M	L	NCM	3084.750	1.386	45	51.1	65.0	19.7	−0.1530
10	75	6	M	L	NCM	1852.875	0.780	57	96.6	100.0	73.7	0.3050
11	66	5	M	L	NCM	290.250	0.000	57	63.4	92.5	98.2	0.2507
12	44	8	M	L	NCM	11,994.750	13.605	36	78.6	81.0	5.1	−0.0993
13	36	20	M	R	NCM	492.750	3.707	54	81.9	93.0	31.0	0.1244
14	59	165	F	L	NCM	14,846.625	16.118	29	18.2	68.0	0.0	−0.3477
15	43	20	F	R	NCM	20,476.125	1.121	41	71.0	91.0	31.0	0.0178
16	33	63	M	R	NCM	529.875	2.931	57	71.7	100.0	68.9	0.2378
17	48	7	M	L	NCM	93,528.000	6.724	31	35.3	42.0	0.0	−0.4201
18	53	12	M	R	NCM	8120.250	11.872	48	52.0	91.0	53.0	0.0642
19	18	5	F	L	CM	17,4997.125	0.690	44	27.7	93.0	5.9	−0.1113
20	51	4	M	R	NCM	276.750	2.253	57	64.2	100.0	89.6	0.2681
21	55	9	M	L	NCM	3.375	8.190	19	97.7	100.0	51.3	0.0439

CST, template corticospinal tract acquired from healthy controls; ARAT, Action Research Arm Test; GRIP, grip strength of affected hand given as a % of less affected hand; MI-UL, Motricity Index (upper limb component); NHPT, Nine-Hole Peg Test score of affected side given as a % of less affected side; PC1, first principle component of the four motor test scores (given as normalised values, arbitrary units); F, female; M, male; L, left; R, right; CM, infarcts affecting primary and secondary motor cortices; NCM, infarcts sparing primary and secondary motor cortices.

2.3. DTI data acquisition

DTI data were collected using a 3T Allegra system (Siemens AG, Erlangen, Germany). For each of controls and patients, 68 images were acquired with a single-shot diffusion-weighted echo planar imaging sequence. The data set consisted of 61 images with high diffusion weighting (b value = 1000 s/mm^2) applied along 61 diffusion directions and 7 images with minimal diffusion weighting (b value = 100 s/mm^2). Each image included 2.3 mm thick 60 axial slices of a 96×96 matrix in a 220 mm $\times$ 220 mm field of view, resulting in 2.3 mm^3 isotropic voxels.

2.4. DTI data analysis

Preprocessing, diffusion tensor modelling and CST tracking were performed using FDT v2.0 included in FSL (http://fsl.fmrib.ox.ac.uk/fsl/). Each subject's 68 images were first realigned to the first image to correct for eddy current-induced distortions and simple head motions. At each voxel, a diffusion tensor was modelled and FA was computed from the diffusion tensor. Also, an image with no diffusion weighting (S_0 image) was estimated. By Markov Chain Monte Carlo sampling, distributions of voxel-wise principal diffusion directions were inferred in preparation for probabilistic tractography.

Deformation fields to transform images between the native space of raw images and the standard space were acquired by applying the New Segment toolbox included in SPM8 (http://www.fil.ion.ucl.ac.uk/spm/) to individual subject's S_0 image. By the forward deformation, an image in the native space could be transformed to the standard space, with a change in the voxel size from isotropic 2.3 mm^3 to isotropic 1.5 mm^3.

In CST tracking, one seed mask, two waypoint masks, one target mask and one exclusion mask in individual subject's native space were employed to spatially confine fibres. The seed mask comprised the primary motor cortex (M1), which was defined to include voxels covering approximately the caudal half of the precentral gyrus along the anterior wall of the central sulcus, based on the Harvard–Oxford Atlas in the standard space. The M1 mask image in the standard space was transformed into individual subject's native space by the inverse deformation. The PLIC and upper and lower pons ipsilateral to the M1 were manually delineated in individual subject's native space, of which the PLIC and upper pons served as the waypoint masks and the lower pons as the target mask. The PLIC mask was placed from the level of the anterior commissure to the base of the corona radiata, and the upper and lower pons masks were located to only include the anterior pons. The corpus callosum and cerebellum were used as the exclusion mask to remove inter-hemispheric and cerebellar trajectories.

By repetitively computing 5000 streamlines starting from every voxel of the seed mask, a distribution of streamline locations from the seed mask to the target mask via the waypoint masks was estimated. In the connectivity distribution, each voxel had a streamline count which passed through the voxel. Each subject's connectivity distribution image was then transformed into the standard space by the forward deformation.

2.5. CST determination

The CST template was generated from 23 controls' connectivity distributions in the standard space. Each control's connectivity distribution was binarised at a threshold of 5% of the maximum voxel value to remove improbable pathways and was then superposed to yield voxel-wise overlap counts. The group-level overlap was binarised at a threshold of half of the number of controls to serve as the CST template. Each patient's CST was acquired by thresholding individual connectivity distribution in the standard space at 5% of the maximum voxel value to remove improbable pathways. It is notable that both the template CST and patient CST were defined in the standard space.

2.6. FA metrics computation

Each patient's FA image was transformed into the standard space by the forward deformation. FA metrics were computed in terms of four measures over the whole tract ($FA_{ipsi,CST}$, $FA_{contra,CST}$, $FA_{ratio,CST}$ and $FA_{asymmetry,CST}$) and tract section comprising the PLIC ($FA_{ipsi,PLIC}$, $FA_{contra,PLIC}$, $FA_{ratio,PLIC}$ and $FA_{asymmetry,PLIC}$) in the template CST and patient CST respectively.

The spatial extent of the whole tract comprised all voxels within the CST in the standard space. A PLIC tract section was defined as three consecutive axial slices along the CST z coordinates of which ranged from 4.5 mm to 7.5 mm in the standard space. The tract section included the mid-posterior portion of the PLIC at the mid-thalamic level which was shown to be the most probable PLIC level within the CST (Kim et al., 2008).

Absolute measures, FA_{ipsi} and FA_{contra}, were computed as the mean of voxel-wise FA within either the whole tract or PLIC tract section in the ipsilesional and contralesional sides, respectively. Relative measures, FA_{ratio} and $FA_{asymmetry}$, were computed as a ratio (FA_{ipsi}/FA_{contra}) and a difference ($(FA_{contra} - FA_{ipsi})/(FA_{contra} + FA_{ipsi})$), respectively, of the two absolute measures.

2.7. FA metrics comparison

Comparisons of patients' FA metrics calculated either from the template CST or patient CST were performed with respect to (1) the inter-tract relation (Fig. 1A), (2) relation to controls' FA metrics (Fig. 1B) and (3) association with post-stroke motor ability (Fig. 1C). Firstly, the inter-tract relation of patients' FA metrics was sought with paired samples t-tests and correlations of FA metrics between the two tracts. Secondly, the comparison of patients' FA metrics from either CST with controls' FA metrics was performed with two samples t-tests of FA metrics between the two groups. Thirdly, the association of patients' FA metrics from either CST with motor ability was assessed with correlations between FA metrics and the PC1 of motor test scores. Motor ability correlations were compared between the template CST and patient CST with Fisher's z transformation. In all statistical inferences, the significance level was set at a p value of 0.05.

Further, to check effects of a wide selection of tract sections as ROIs, we acquired distributions of correlation coefficients between patients' FA metrics and motor ability along each tract. Similar to the PLIC tract section, each tract section was determined as three consecutive slices along the CST. In the range of z coordinates from -31.5 mm to 45 mm in the standard space, 52 tract sections were considered, with two consecutive tract sections overlapped by two slices.

Additionally, we estimated the degree of variability in the patient CST by a spatial distance between the template CST and patient CST in each hemisphere and assessed relationships of the variability in the patient CST with (i) motor ability and (ii) FA metrics in patients. In each slice with the same z coordinate in the standard space, centre coordinates of the two tracts were found and the distance between them was measured. In each patient, the distance between the two tracts was acquired as the mean of slice-wise distances. We correlated the variability in the patient CST with the PC1 of motor test scores and also with FA metric differences between the template CST and patient CST.

3. Results

3.1. Template CST and patient CST

The template CST which was constructed separately for left and right sides is shown in Fig. 2A. The overlap of individual patients' CSTs is displayed in Fig. 2B. The overlap in the left panel of Fig. 2B was acquired from patients with left hemisphere lesions and the

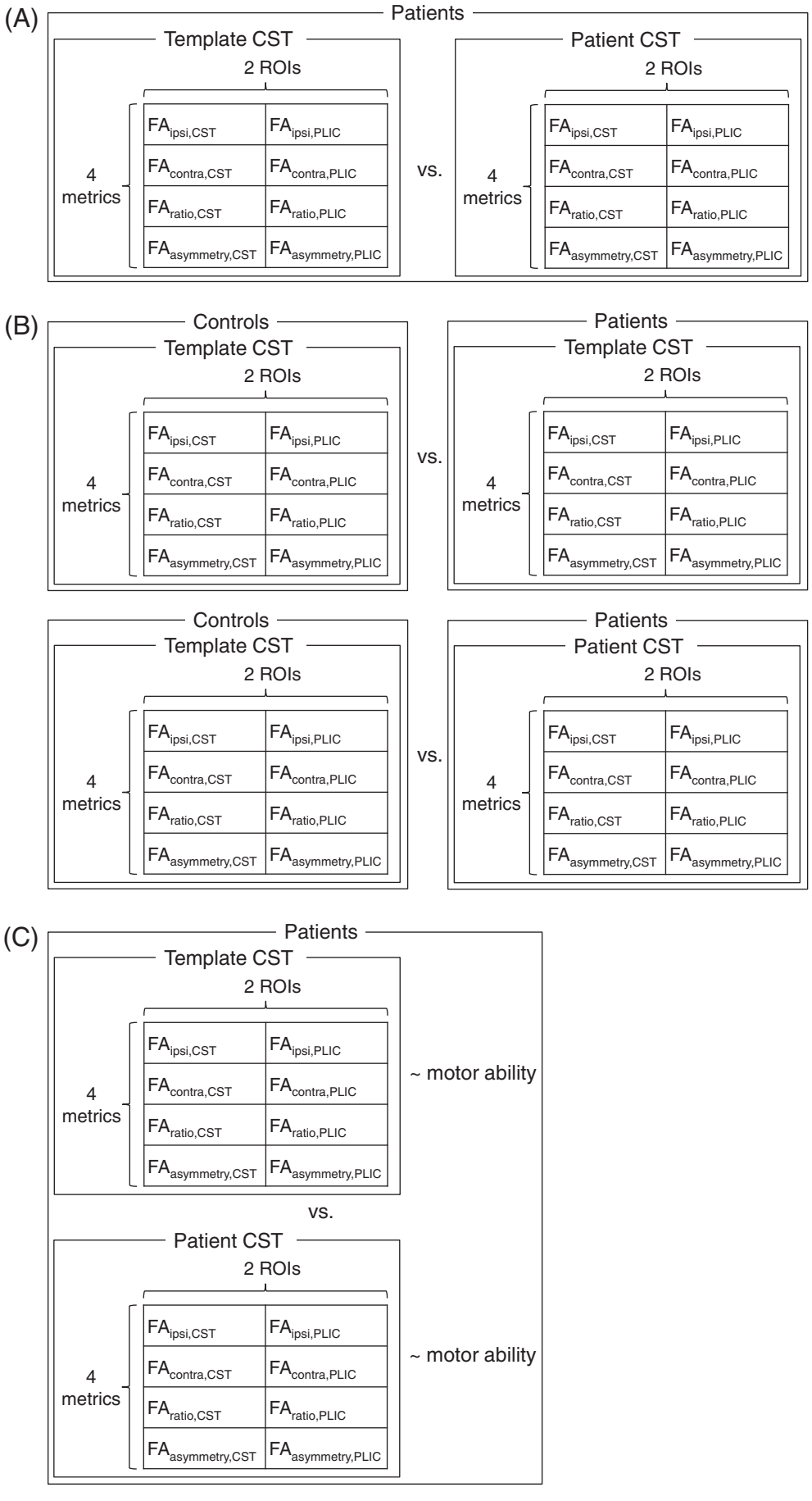
(A)
Patients
Template CST
2 ROIs
4 metrics
FA ipsi,CST
FA ipsi,PLIC
FA contra,CST
FA contra,PLIC
FA ratio,CST
FA ratio,PLIC
FA asymmetry,CST
FA asymmetry,PLIC
vs.
Patient CST
2 ROIs
4 metrics
FA ipsi,CST
FA ipsi,PLIC
FA contra,CST
FA contra,PLIC
FA ratio,CST
FA ratio,PLIC
FA asymmetry,CST
FA asymmetry,PLIC
(B)
Controls
Template CST
2 ROIs
4 metrics
FA ipsi,CST
FA ipsi,PLIC
FA contra,CST
FA contra,PLIC
FA ratio,CST
FA ratio,PLIC
FA asymmetry,CST
FA asymmetry,PLIC
vs.
Patients
Template CST
2 ROIs
4 metrics
FA ipsi,CST
FA ipsi,PLIC
FA contra,CST
FA contra,PLIC
FA ratio,CST
FA ratio,PLIC
FA asymmetry,CST
FA asymmetry,PLIC
Controls
Template CST
2 ROIs
4 metrics
FA ipsi,CST
FA ipsi,PLIC
FA contra,CST
FA contra,PLIC
FA ratio,CST
FA ratio,PLIC
FA asymmetry,CST
FA asymmetry,PLIC
vs.
Patients
Patient CST
2 ROIs
4 metrics
FA ipsi,CST
FA ipsi,PLIC
FA contra,CST
FA contra,PLIC
FA ratio,CST
FA ratio,PLIC
FA asymmetry,CST
FA asymmetry,PLIC
(C)
Patients
Template CST
2 ROIs
4 metrics
FA ipsi,CST
FA ipsi,PLIC
FA contra,CST
FA contra,PLIC
FA ratio,CST
FA ratio,PLIC
FA asymmetry,CST
FA asymmetry,PLIC
~ motor ability
vs.
Patient CST
2 ROIs
4 metrics
FA ipsi,CST
FA ipsi,PLIC
FA contra,CST
FA contra,PLIC
FA ratio,CST
FA ratio,PLIC
FA asymmetry,CST
FA asymmetry,PLIC
~ motor ability

overlap in the right panel of Fig. 2B was acquired from patients with right hemisphere lesions.

3.2. Within-patients comparison of FA metrics

We compared patients' FA metrics calculated from the template CST and patient CST. There were no differences in FA metrics between the two tracts for either of the two ROIs (whole tract and PLIC), except $FA_{contra,CST}$ which was greater when using the template CST ($t(20) = 5.3860$, p value < 0.0001) (Fig. 3). Further, when we compared patients' FA metrics calculated from the template CST and patient CST, we found positive correlations for $FA_{ipsi,CST}$ ($r = 0.7114$, p value $= 0.0003$), $FA_{ipsi,PLIC}$ ($r = 0.8034$, p value < 0.0001), $FA_{contra,CST}$ ($r = 0.6366$, p value $= 0.0019$), $FA_{contra,PLIC}$ ($r = 0.5119$, p value $= 0.0177$), $FA_{ratio,CST}$ ($r = 0.5900$, p value $= 0.0049$), $FA_{ratio,PLIC}$ ($r = 0.7179$, p value $= 0.0002$), $FA_{asymmetry,CST}$ ($r = 0.5881$, p value $= 0.0050$) and $FA_{asymmetry,PLIC}$ ($r = 0.6949$, p value $= 0.0005$) (Fig. 4). In summary, CST integrity values calculated from the template CST corresponded well with those calculated from patient CST.

3.3. Between-groups comparison of FA metrics

We compared controls' FA metrics on the template CST with (i) patients' FA metrics on the template CST and (ii) patients' FA metrics on the patient CST. For the first comparison (controls on the template CST versus patients on the template CST), the following were different between the two groups; $FA_{ipsi,CST}$ ($t(42) = 5.7339$, p value < 0.0001), $FA_{ipsi,PLIC}$ ($t(42) = 3.331$, p value $= 0.0018$), $FA_{contra,CST}$ ($t(42) = 3.3949$, p value $= 0.0015$), $FA_{ratio,CST}$ ($t(42) = 4.2093$, p value $= 0.0001$), $FA_{ratio,PLIC}$ ($t(42) = 2.7011$, p value $= 0.0099$), $FA_{asymmetry,CST}$ ($t(42) = -3.9645$, p value $= 0.0003$) and $FA_{asymmetry,PLIC}$ ($t(42) = -2.7907$, p value $= 0.0079$), whereas $FA_{contra,PLIC}$ was not (Fig. 5). For the second comparison (controls on the template CST versus patients on the patient CST), the following were different between the two groups; $FA_{ipsi,CST}$ ($t(42) = 8.3110$, p value < 0.0001), $FA_{ipsi,PLIC}$ ($t(42) = 3.3676$, p value $= 0.0016$), $FA_{contra,CST}$ ($t(42) = 6.3948$, p value < 0.0001), $FA_{ratio,CST}$ ($t(42) = 3.1203$, p value $= 0.0033$), $FA_{ratio,PLIC}$ ($t(42) = 3.2365$, p value $= 0.0024$), $FA_{asymmetry,CST}$ ($t(42) = -3.4372$, p value $= 0.0013$) and $FA_{asymmetry,PLIC}$ ($t(42) = -3.4245$, p value $= 0.0014$), wheras $FA_{contra,PLIC}$ once again was not (Fig. 6). In general, there was strong evidence of diminished CST integrity in ipsilesional CST integrity together with increased asymmetry in patients compared to controls. Contralesional CST integrity was diminished in patients when assessed over the whole tract, but not over the PLIC tract section.

3.4. Correlation of FA metrics with motor ability

We examined for correlations between patients' FA metrics (either from the template CST or patient CST) with motor ability as assessed by the PC1 of motor test scores. When using the template CST, greater motor ability was seen in those with greater ipsilesional CST integrity as assessed with $FA_{ipsi,CST}$ ($r = 0.4861$, p value $= 0.0255$), $FA_{ipsi,PLIC}$ ($r = 0.5667$, p value $= 0.0074$), $FA_{ratio,CST}$ ($r = 0.5195$, p value $= 0.0158$), $FA_{ratio,PLIC}$ ($r = 0.5575$, p value $= 0.0086$), $FA_{asymmetry,CST}$ ($r = -0.5176$, p value $= 0.0163$) and $FA_{asymmetry,PLIC}$ ($r = -0.5687$, p value $= 0.0071$). When using patient CST, greater motor ability was also seen in those with greater ipsilesional CST integrity as assessed with $FA_{ipsi,CST}$ ($r = 0.5376$, p value $= 0.0120$), $FA_{ipsi,PLIC}$ ($r = 0.5019$, p value $= 0.0204$), $FA_{ratio,CST}$ ($r = 0.6071$, p value $= 0.0035$), $FA_{ratio,PLIC}$ ($r = 0.4376$, p value $= 0.0473$), $FA_{asymmetry,CST}$ ($r = -0.6065$, p value $= 0.0036$) and $FA_{asymmetry,PLIC}$ ($r = -0.4734$, p value $= 0.0302$). That is, patients' FA_{ipsi}, FA_{ratio} and $FA_{asymmetry}$ calculated with either tract correlated positively with motor ability in chronic stroke patients, whereas FA_{contra} did not (Fig. 7). Further, when we compared correlation coefficients between the two tracts, there were no differences in the strength of correlation.

3.5. Tract-wide distribution of motor ability correlation

We examined for correlations between motor ability and patients' FA metrics not only in the PLIC tract section, but also in every tract section along the tract. For both the template CST and patient CST, patients' FA_{ipsi}, FA_{ratio} and $FA_{asymmetry}$ correlated with the PC1 of motor test scores across a wide range of tract sections beyond the PLIC tract section, while FA_{contra} was less consistent (Fig. 8).

3.6. Variability in the patient CST

The motivation for proposing the use of the template CST in assessing CST damage after stroke is related to the variability in the CST when determined by tractography in individual patients. We attempted to characterise the variability in the patient CST in terms of its relation to motor ability and FA metrics. When assessed using the whole tract, the ipsilesional inter-tract distances correlated with the PC1 of motor test scores (p value $= 0.0078$) in that greater separation between template and patient CST was associated with worse motor ability (Supplementary Fig. 1). This did not hold true for inter-tract distances from just ipsilesional PLIC, nor for contralesional tract with either ROI (Supplementary Fig. 1). There was no correlation between inter-tract distances with differences in FA metrics (between the template and patient CST) for any method (Supplementary Fig. 2).

4. Discussion

The wide-scale use of CST measurement to improve prediction of outcome or response to therapy requires an approach which is feasible and reproducible across stroke centres. Here we have compared the use of a standard CST template derived from healthy volunteers in place of CSTs from individual stroke patients. Tract-based ROIs, such as the whole tract and PLIC tract section, were defined using the standard CST template and could be commonly applied to every patient. We found that a range of FA-based metrics thought to reflect CST integrity, were not significantly altered by the use of a standard template.

In this study, we considered stroke patients with a wide range of infarct sizes and levels of motor ability post-stroke (Table 1). The size of the infarct varied between 3.4 mm^3 and 174997.1 mm^3 and the lesion load of the template CST ranged from 0.0% to 29.9%. With respect to location, patients with combined cortical/subcortical as well as subcortical infarcts were included. The degree of motor impairment also varied considerably. This diversity of patient characteristics suggests that the CST template approach could be applied widely. Creation of CSTs in individual stroke patients is problematic due to the inability to track through the lesion itself, as well as loss of structural integrity due to secondary degeneration (Carter et al., 2012; Liang et al., 2007). The template CST could be used to define tract-based ROIs with which to evaluate FA metrics even

Fig. 1. Overview of the approach to comparing the performance between the template corticospinal tract (CST) and patient CST in evaluating patients' fractional anisotropy (FA) metrics. Four FA metrics over two regions of interests (ROIs), including the whole tract ($FA_{ipsi,CST}$, $FA_{contra,CST}$, $FA_{ratio,CST}$ and $FA_{asymmetry,CST}$) and tract section comprising the posterior limb of the internal capsule ($FA_{ipsi,PLIC}$, $FA_{contra,PLIC}$, $FA_{ratio,PLIC}$ and $FA_{asymmetry,PLIC}$), were considered. Patients' FA metrics (A) were compared between the two tracts, (B) were compared with controls' FA metrics and (C) correlated with motor ability and the correlation was compared between the two tracts.

in patients whose CST reconstruction failed. This approach has also allowed initial investigations into the functional consequences of damage to CST originating from secondary cortical motor areas (e.g. dorsal and ventral premotor cortices and supplementary motor area) (Newton et al., 2006) and to tracts originating from specific body regions (e.g. upper limb) (Schulz et al., 2012). Furthermore, CST templates could be subdivided based on the somatotopic organisation of fibres in the brainstem (Hong et al., 2010; Kwon et al., 2011; Lee et al., 2012) allowing clearer structure–function relationships to be determined.

Previous work has suggested that the trajectory of the CST can change after stroke (Jang, 2011). This might lead to an alteration in the route of the tracked CST in the chronic stroke phase so that it becomes quite distant from the healthy CST. Our results suggest that the average CST in stroke patients, especially on the ipsilesional side, is more variable compared to the template CST (Fig. 2). Specifically the variability in the patient CST correlated with motor ability (Supplementary Fig. 1). To address this potential confound, we examined whether the degree of deviation of the patient CST from the template CST was related to the difference in FA metrics measured in the two tracts. However, not only did we not find a difference between FA metrics (FA_{ipsi}, FA_{ratio} and $FA_{asymmetry}$) in the two tracts (Fig. 3), but neither was there a correlation between differences in FA metrics and spatial distances (Supplementary Fig. 2). Furthermore, FA metrics from the two tracts generally correlated with each other (Fig. 4). These results suggest that our findings are not contaminated by unusual post-stroke CST trajectories.

We have looked for relationships between metrics of CST integrity and motor ability in a cross sectional analysis of chronic stroke patients. We suggest that our results support the future use of standard CST templates in assessment of CST integrity for the purposes of predicting motor outcomes. However, this would necessitate early imaging data being used to predict future levels of impairment. Although FA metrics acquired one to two weeks after stroke have been used to predict motor outcome (Liu et al., 2012; Yu et al., 2009), it is reasonable to ask whether FA changes distant from the primary lesion or whole tract FA will be affected in the early phase to the degree that it is in the chronic phase.

Our results showed that there was no statistical difference between a number of approaches to examining the correlation between CST integrity and motor ability. However, some trends are worth pointing out. The correlation coefficient was consistently larger when using the PLIC tract section from the template CST, but was larger when using the whole tract from the patient CST (Fig. 7). This might be attributable to the finding that the correlations between FA metrics and motor ability are seen across a wider range of axial sections, particularly below the PLIC, when using the patient CST (Fig. 8). However, this result suggests that as a variable to account for motor ability, PLIC FA values are reasonably robust to alterations in location of axial section (particularly *z* coordinates between 0 mm and 25 mm).

In comparison to controls, all of FA_{ipsi}, FA_{ratio} and $FA_{asymmetry}$ are considered robust FA metrics which indicate diminished structural integrity in the ipsilesional side after stroke, irrespective of whether the whole tract or PLIC tract section is used as an ROI (A, C and D in Figs. 5 and 6). Only FA_{cont} was affected by the ROIs in such a way that it was different from controls in the whole tract but not in the PLIC tract section (B in Figs. 5 and 6). Although this reflects tract-wide degeneration even on the contralesional side, it does not seem to be severe enough to affect relative measures such as FA_{ratio} and $FA_{asymmetry}$, suggesting that these approaches can still detect lesion induced differences in patient groups. Degeneration even on the contralesional side may be due to secondary degeneration occurring in remote regions connected through fibre pathways with the primary damage on the ipsilesional side (Crofts et al., 2011).

With regard to the standardised approach using the template CST, there are a number of unresolved issues. Firstly, general applicability of the template CST approach might need to be tested in specific groups of patients, such as those with very large lesions. Secondly, broad adoption of this type of approach will require that fully automated processes such as spatial normalisation are as accurate as possible. It is acknowledged that spatial preprocessing is not perfect. For example, automated normalisation can lead to lesion size reduction (Ripollés et al., 2012). Thirdly, there are still limitations in tractography which apply equally to the creation of standard CST templates. Specifically, partial volume effects due to limitation of spatial resolution of DTI data (Alexander et al., 2001) and fibre crossing in determining tracking direction (Wiegell et al., 2000) are well known. Advances in the techniques for DTI data acquisition and tractography are likely to lead to improvements in construction of the template CST.

There are a number of potential practical applications of template tracts. Firstly, as shown in this study, a study-specific template tract could be created from healthy subjects who match patients of interest in their characteristics such as age. Secondly, one might envisage standard template tracts being created from a very large number of healthy subjects who generally match the patient group of interest. This approach would be more suited to studies in which assessment of integrity specific white matter tracts such as CST needs to be measured across several centres. Our results here suggest that further work in this direction is warranted in order to achieve this goal. For example, one approach might be to create a mask that constrains the extent of the tract using a mean FA skeleton mask generated using tract-based spatial statistics (Smith et al., 2006) as has been used by

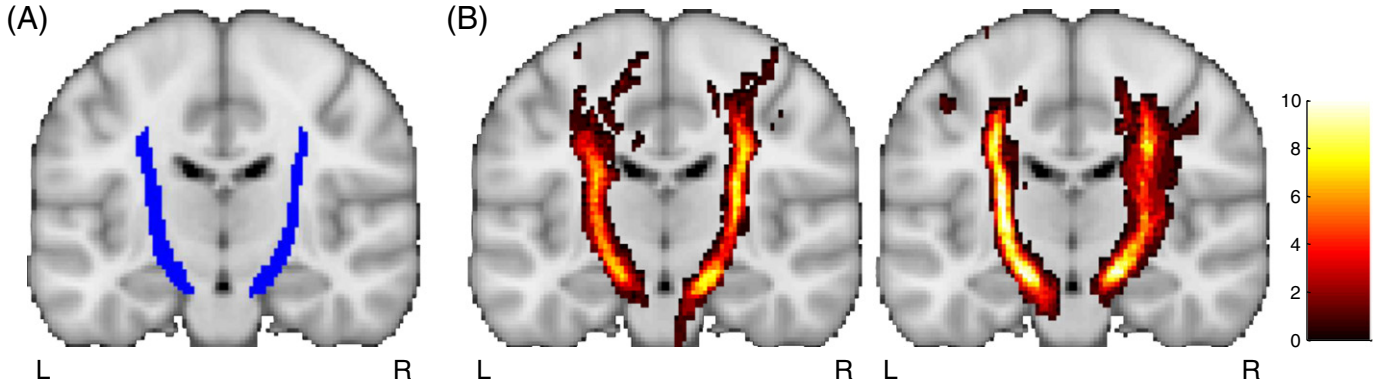

Fig. 2. (A) The template corticospinal tract (CST) acquired from healthy controls and (B) the overlap of CSTs for patients with left hemisphere lesions (left panel) and patients with right hemisphere lesions (right panel). In (B), the colour of each voxel corresponds to the degree of superposition across patients. L, left; R, right.

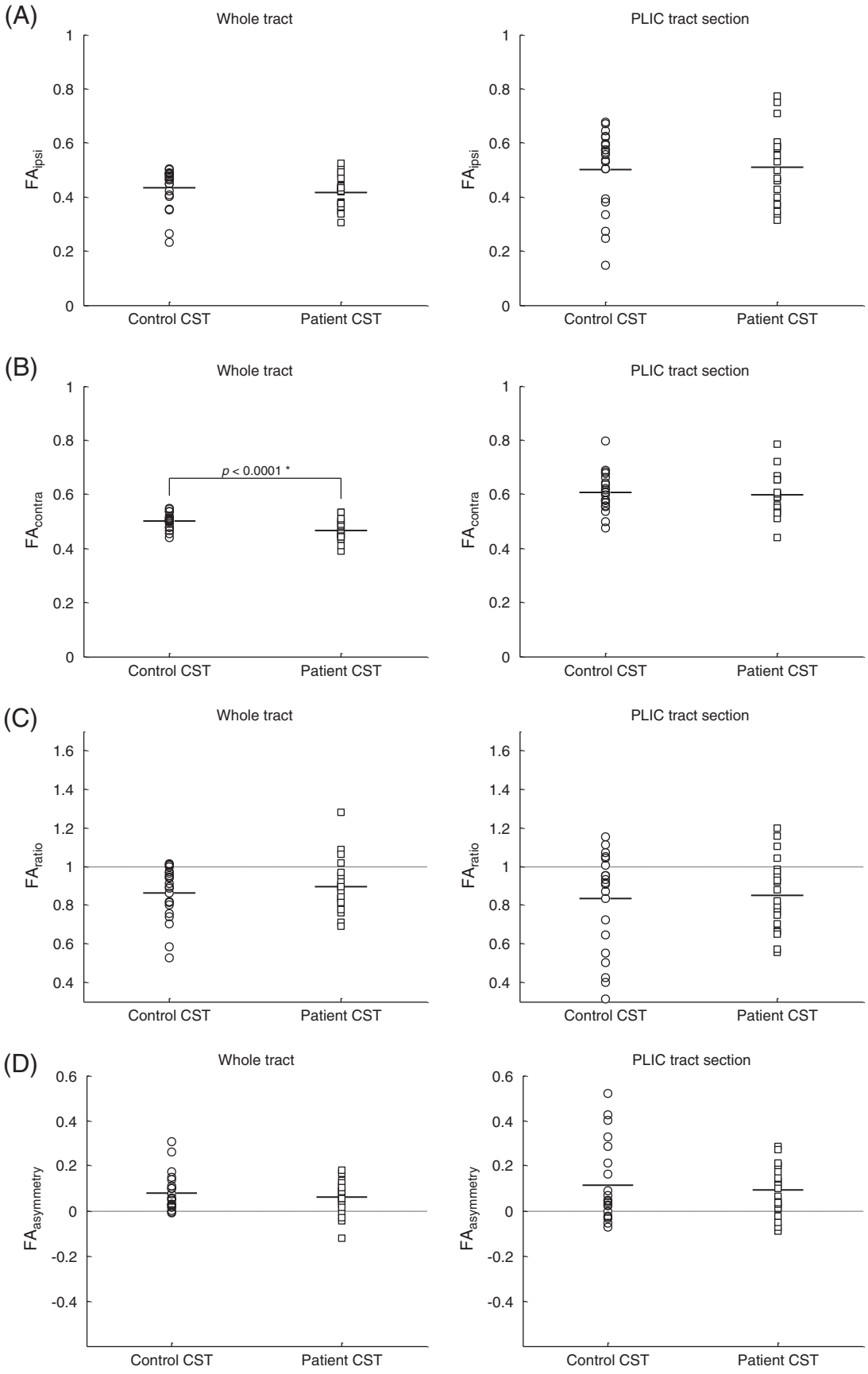

Fig. 3. Comparisons of patients' fractional anisotropy (FA) metrics between the template corticospinal tract (CST) and patient CST. FA metrics include (A) FA in the ipsilesional side (FA_{ipsi}), (B) FA in the contralesional side (FA_{contra}), (C) FA ratio of the ipsilesional side to the contralesional side (FA_{ratio}) and (D) FA asymmetry between the contralesional and ipsilesional sides ($FA_{asymmetry}$). Regions of interest are the whole tract (left panels) and posterior limb of the internal capsule (PLIC) tract section (right panels). The range of a vertical axis was matched between comparisons in each row. *p*, *p* value; *, statistical significance.

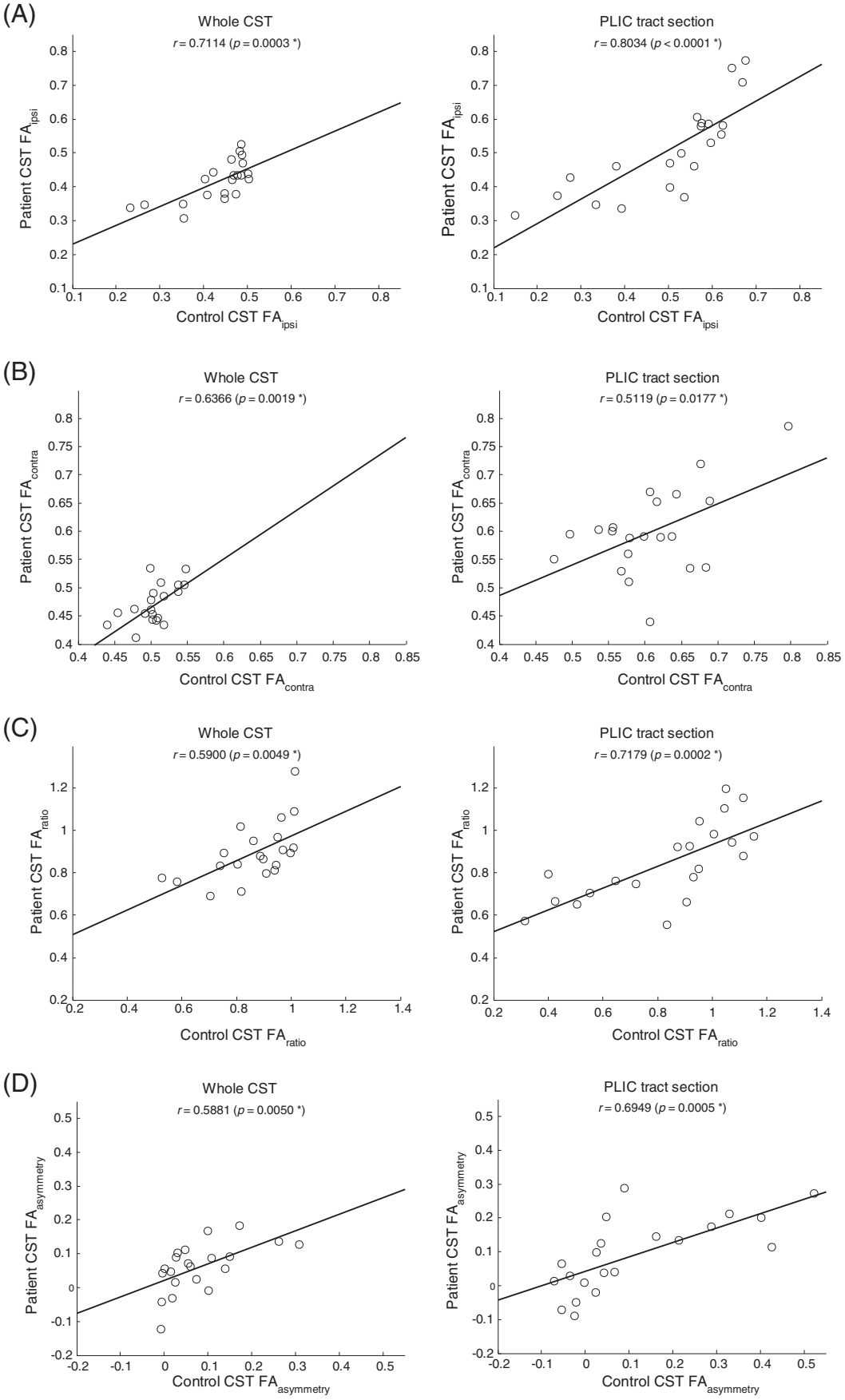

Fig. 4. Correlations of patients' fractional anisotropy (FA) metrics between the template corticospinal tract (CST) and patient CST. FA metrics include (A) FA in the ipsilesional side (FA_{ipsi}), (B) FA in the contralesional side (FA_{contra}), (C) FA ratio of the ipsilesional side to the contralesional side (FA_{ratio}) and (D) FA asymmetry between the contralesional and ipsilesional sides ($FA_{asymmetry}$). Regions of interest are the whole tract (left panels) and posterior limb of the internal capsule (PLIC) tract section (right panels). Solid lines indicate linear fits in case of statistically significant correlations. The ranges of horizontal and vertical axes were matched between correlations in each row. *p*, *p* value; *, statistical significance.

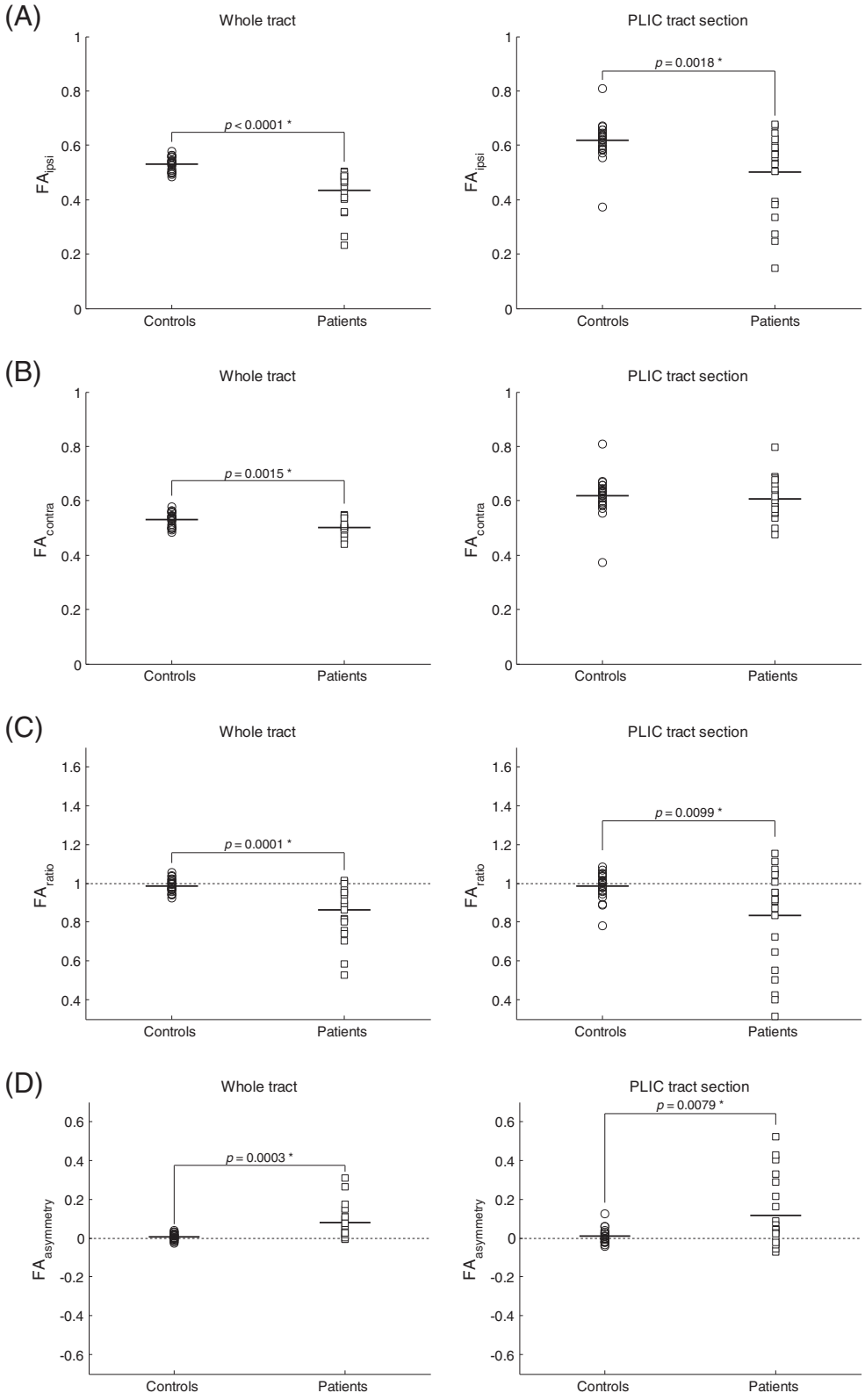

Fig. 5. Comparisons of patients' fractional anisotropy (FA) metrics on the template corticospinal tract (CST) and healthy controls' FA metrics on the template CST. FA metrics include (A) FA in the ipsilesional side (FA_{ipsi}), (B) FA in the contralesional side (FA_{contra}), (C) FA ratio of the ipsilesional side to the contralesional side (FA_{ratio}) and (D) FA asymmetry between the contralesional and ipsilesional sides ($FA_{asymmetry}$). Regions of interest are the whole tract (left panels) and posterior limb of the internal capsule (PLIC) tract section (right panels). The range of a vertical axis was matched between comparisons in each row. *p*, *p* value; *, statistical significance.

others (Squarcina et al., 2012). The white matter skeleton mask would alleviate partial volume effects at the edges of the tract by focusing on the alignment–invariant tract representation. Alternatively, the use of a template tract with weighted values, acquired as a group probability map (Riley et al., 2011), could also be effective for focusing on central voxels along the tract.

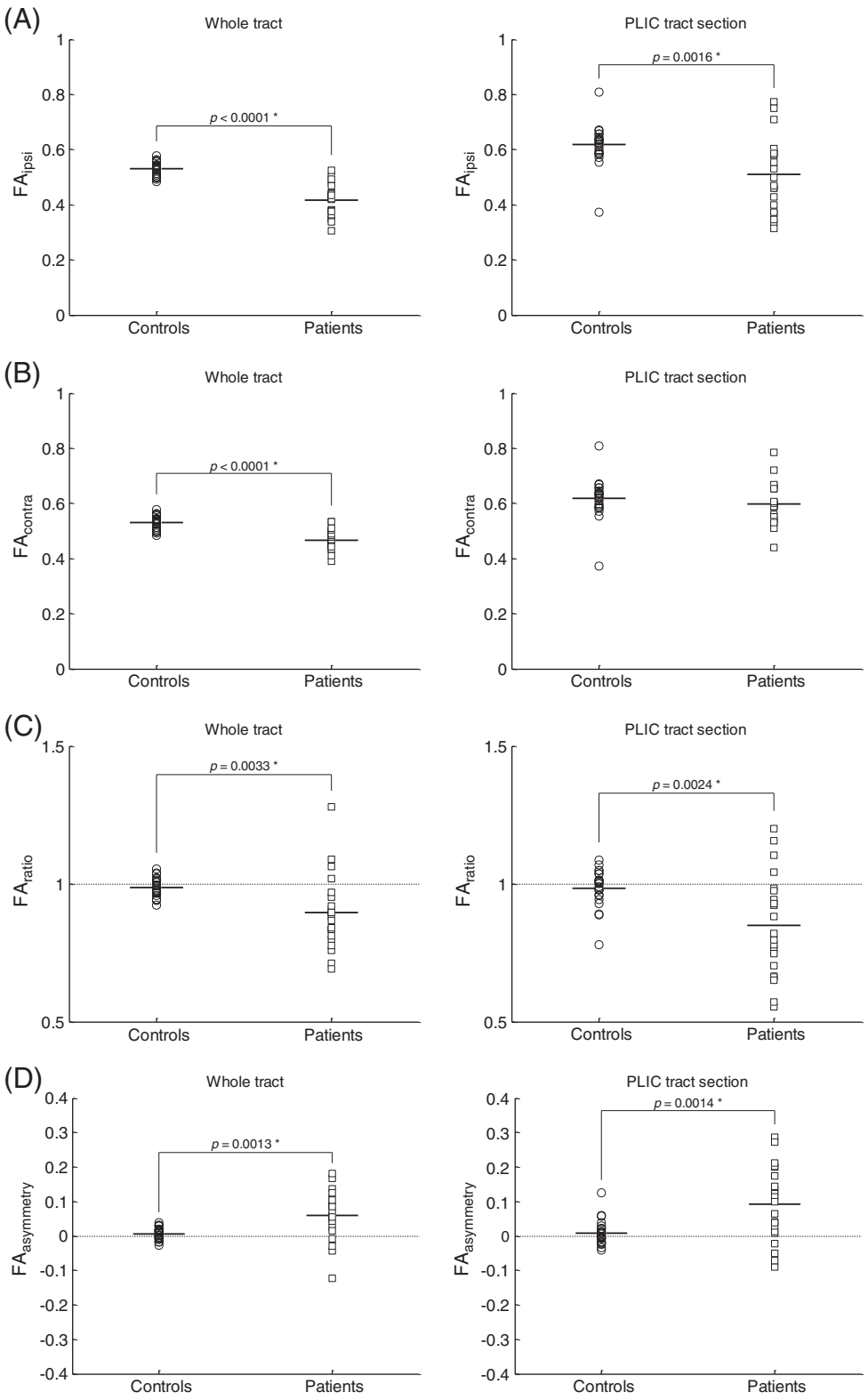

Fig. 6. Comparisons of patients' fractional anisotropy (FA) metrics on the patient corticospinal tract (CST) and healthy controls' FA metrics on the template CST. FA metrics include (A) FA in the ipsilesional side (FA_{ipsi}), (B) FA in the contralesional side (FA_{contra}), (C) FA ratio of the ipsilesional side to the contralesional side (FA_{ratio}) and (D) FA asymmetry between the contralesional and ipsilesional sides ($FA_{asymmetry}$). Regions of interest are the whole tract (left panels) and posterior limb of the internal capsule (PLIC) tract section (right panels). The range of a vertical axis was matched between comparisons in each row. *p*, *p* value; *, statistical significance.

In summary, in spite of interactions related to different measures (FA_{ipsi}, FA_{cont}, FA_{ratio} and $FA_{asymmetry}$) and ROIs (part and whole of the CST), the CST template acquired from healthy subjects was comparable to the CST acquired from patients in the evaluation of FA metrics in chronic stroke. This finding suggests the feasibility of replacement of the patient CST with the template CST for the assessment of altered

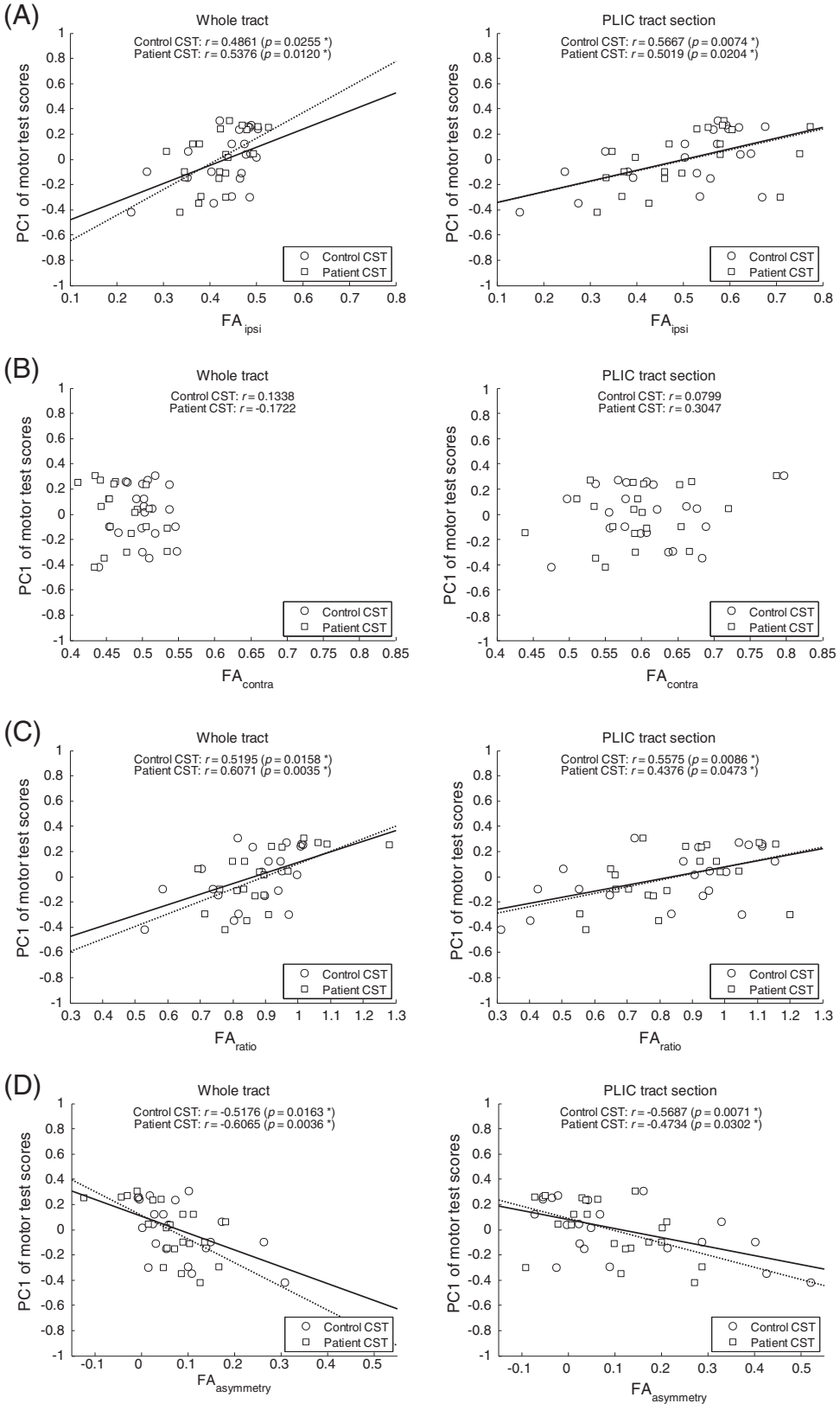

Fig. 7. Correlations of patients' fractional anisotropy (FA) metrics with motor ability, as represented by the first principal component (PC1) of motor test scores. Patients' fractional anisotropy (FA) metrics were evaluated on each of the template corticospinal tract (CST) and patient CST. FA metrics include (A) FA in the ipsilesional side (FA_{ipsi}), (B) FA in the contralesional side (FA_{contra}), (C) FA ratio of the ipsilesional side to the contralesional side (FA_{ratio}) and (D) FA asymmetry between the contralesional and ipsilesional sides ($FA_{asymmetry}$). Regions of interest are the whole tract (left panels) and posterior limb of the internal capsule (PLIC) tract section (right panels). Solid and dotted lines indicate linear fits in case of statistically significant correlations for the template CST and patient CST respectively. The range of a horizontal axis was matched between correlations in each row. *r*, correlation coefficient; *p*, *p* value; *, statistical significance.

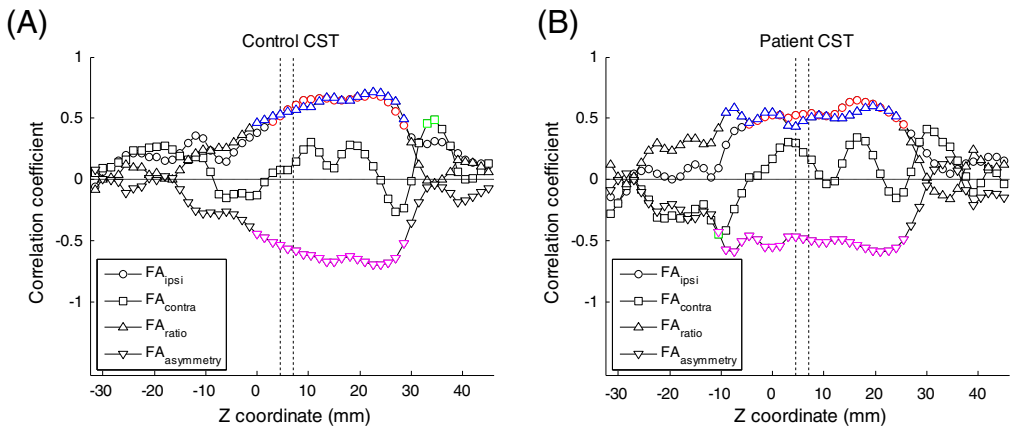

Fig. 8. Distributions of motor ability correlations of patients' fractional anisotropy (FA) metrics in every tract section along (A) the template corticospinal tract (CST) and (B) patient CST. The *z* coordinates of the 52 tract sections range from -31.5 mm to 45 mm in the MNI space. FA metrics include FA in the ipsilesional side (FA_{ipsi}), FA in the contralesional side (FA_{contra}), FA ratio of the ipsilesional side to the contralesional side (FA_{ratio}) and FA asymmetry between the contralesional and ipsilesional sides ($FA_{asymmetry}$). The two vertical dotted lines indicate the range of *z* coordinates from 4.5 mm to 7.5 mm, which corresponds to the tract section comprising the posterior limb of the internal capsule. Red circles, blue squares, green upward triangles and pink downward triangles mean statistically significant correlations for FA_{ipsi}, FA_{contra}, FA_{ratio} and $FA_{asymmetry}$ respectively.

structural integrity after stroke. CST template-based automated quantification will be a methodologically sound and more objective approach to facilitate clinical applications.

Supplementary data to this article can be found online at http://dx.doi.org/10.1016/j.nicl.2013.04.002.

Acknowledgements

This work was supported by The Wellcome Trust (no. 088414) (NW, CHP), the European Commission under the 7th Framework Programme – HEALTH – Collaborative Project Plasticise (no. 223524) and the Canadian Institute of Health Research (MHB). Scanning was performed at The Wellcome Trust Centre for Neuroimaging which is supported by core funding from the Wellcome Trust (no. 091593/Z/10/Z).

References

Alexander, A.L., Hasan, K.M., Lazar, M., Tsuruda, J.S., Parker, D.L., 2001. Analysis of partial volume effects in diffusion-tensor MRI. Magnetic Resonance in Medicine 45, 770–780.
Basser, P.J., Pierpaoli, C., 1996. Microstructural and physiological features of tissues elucidated by quantitative-diffusion-tensor MRI. Journal of Magnetic Resonance. Series B 111, 209–219.
Bohannon, R.W., 1999. Motricity index scores are valid indicators of paretic upper extremity strength following stroke. Journal of Physical Therapy Science 11, 59–61.
Borich, M.R., Wadden, K.P., Boyd, L.A., 2012. Establishing the reproducibility of two approaches to quantify white matter tract integrity in stroke. NeuroImage 59, 2393–2400.
Carter, A.R., Patel, K.R., Astafiev, S.V., Snyder, A.Z., Rengachary, J., Strube, M.J., Pope, A., Shimony, J.S., Lang, C.E., Shulman, G.L., Corbetta, M., 2012. Upstream dysfunction of somatomotor functional connectivity after corticospinal damage in stroke. Neurorehabilitation and Neural Repair 26, 7–19.
Crofts, J.J., Higham, D.J., Bosnell, R., Jbabdi, S., Matthews, P.M., Behrens, T.E.J., Johansen-Berg, H., 2011. Network analysis detects changes in the contralesional hemisphere following stroke. NeuroImage 54, 161–169.
Globas, C., Lam, J.M., Zhang, W., Imanbayev, A., Hertler, B., Becker, C., Whitall, J., McCombe-Waller, S., Mori, S., Hanley, D.F., Luft, A.R., 2011. Mesencephalic corticospinal atrophy predicts baseline deficit but not response to unilateral or bilateral arm training in chronic stroke. Neurorehabilitation and Neural Repair 25, 81–87.
Hong, Y.H., Sung, J.J., Kim, S.M., Park, K.S., Lee, K.W., Chang, K.H., Song, I.C., 2008. Diffusion tensor tractography-based analysis of the pyramidal tract in patients with amyotrophic lateral sclerosis. Journal of Neuroimaging 18, 282–287.
Hong, J.H., Son, S.M., Jang, S.H., 2010. Somatotopic location of corticospinal tract at pons in human brain: a diffusion tensor tractography study. NeuroImage 51, 952–955.
Jang, S.H., 2011. A review of diffusion tensor imaging studies on motor recovery mechanisms in stroke patients. NeuroRehabilitation 28, 345–352.
Jang, S.H., Cho, S.H., Kim, Y.H., Han, B.S., Byun, W.M., Son, S.M., Kim, S.H., Lee, S.J., 2005. Diffusion anisotrophy in the early stages of stroke can predict motor outcome. Restorative Neurology and Neuroscience 23, 11–17.
Jang, S.H., Woo, M.B., Bong, S.H., Park, H.J., Bai, D., Young, H.A., Kwon, Y.H., Mi, Y.L., 2006. Recovery of a partially damaged corticospinal tract in a patient with intracerebral hemorrhage: a diffusion tensor image study. Restorative Neurology and Neuroscience 24, 25–29.
Jayaram, G., Stagg, C.J., Esser, P., Kischka, U., Stinear, J., Johansen-Berg, H., 2012. Relationships between functional and structural corticospinal tract integrity and walking post stroke. Clinical Neurophysiology 123, 2422–2428.
Kellor, M., Frost, J., Silberberg, N., Iversen, I., Cummings, R., 1971. Hand strength and dexterity. The American Journal of Occupational Therapy: Official Publication of the American Occupational Therapy Association 25, 77–83.
Kim, Y.H., Kim, D.S., Hong, J.H., Park, C.H., Hua, N., Bickart, K.C., Byun, W.M., Jang, S.H., 2008. Corticospinal tract location in internal capsule of human brain: diffusion tensor tractography and functional MRI study. NeuroReport 19, 817–820.
Kwon, H.G., Hong, J.H., Jang, S.H., 2011. Anatomic location and somatotopic arrangement of the corticospinal tract at the cerebral peduncle in the human brain. American Journal of Neuroradiology 32, 2116–2119.
Lee, D.H., Kwon, Y.H., Hwang, Y.T., Kim, J.H., Park, J.W., 2012. Somatotopic location of corticospinal tracts in the internal capsule with MR tractography. European Neurology 67, 69–73.
Liang, Z., Zeng, J., Liu, S., Ling, X., Xu, A., Yu, J., Ling, L., 2007. A prospective study of secondary degeneration following subcortical infarction using diffusion tensor imaging. Journal of Neurology, Neurosurgery, and Psychiatry 78, 581–586.
Lindberg, P.G., Skejø, P.H.B., Rounis, E., Nagy, Z., Schmitz, C., Wernegren, H., Bring, A., Engardt, M., Forssberg, H., Borg, J., 2007. Wallerian degeneration of the corticofugal tracts in chronic stroke: a pilot study relating diffusion tensor imaging, transcranial magnetic stimulation, and hand function. Neurorehabilitation and Neural Repair 21, 551–560.
Lindenberg, R., Renga, V., Zhu, L.L., Betzler, F., Alsop, D., Schlaug, G., 2010. Structural integrity of corticospinal motor fibers predicts motor impairment in chronic stroke. Neurology 74, 280–287.
Lindenberg, R., Zhu, L.L., Rüber, T., Schlaug, G., 2012. Predicting functional motor potential in chronic stroke patients using diffusion tensor imaging. Human Brain Mapping 33, 1040–1051.
Liu, X., Tian, W., Qiu, X., Li, J., Thomson, S., Li, L., Wang, H.Z., 2012. Correlation analysis of quantitative diffusion parameters in ipsilateral cerebral peduncle during wallerian degeneration with motor function outcome after cerebral ischemic stroke. Journal of Neuroimaging 22, 255–260.
Lotze, M., Beutling, W., Loibl, M., Domin, M., Platz, T., Schminke, U., Byblow, W.D., 2012. Contralesional motor cortex activation depends on ipsilesional corticospinal tract integrity in well-recovered subcortical stroke patients. Neurorehabilitation and Neural Repair 26, 594–603.
Lyle, R.C., 1981. A performance test for assessment of upper limb function in physical rehabilitation treatment and research. International Journal of Rehabilitation Research 4, 483–492.
Madhavan, S., Krishnan, C., Jayaraman, A., Rymer, W.Z., Stinear, J.W., 2011. Corticospinal tract integrity correlates with knee extensor weakness in chronic stroke survivors. Clinical Neurophysiology 122, 1588–1594.
Møller, M., Frandsen, J., Andersen, G., Gjedde, A., Vestergaard-Poulsen, P., Østergaard, L., 2007. Dynamic changes in corticospinal tracts after stroke detected by fibretracking. Journal of Neurology, Neurosurgery, and Psychiatry 78, 587–592.
Nelles, M., Gieseke, J., Flacke, S., Lachenmayer, L., Schild, H.H., Urbach, H., 2008. Diffusion tensor pyramidal tractography in patients with anterior choroidal artery infarcts. American Journal of Neuroradiology 29, 488–493.
Newton, J.M., Ward, N.S., Parker, G.J.M., Deichmann, R., Alexander, D.C., Friston, K.J., Frackowiak, R.S.J., 2006. Non-invasive mapping of corticofugal fibres from multiple motor areas — relevance to stroke recovery. Brain 129, 1844–1858.
Partridge, S.C., Mukherjee, P., Berman, J.I., Henry, R.G., Miller, S.P., Lu, Y., Glenn, O.A., Ferriero, D.M., Barkovich, A.J., Vigneron, D.B., 2005. Tractography-based of quantitation of diffusion tensor imaging parameters in white matter tracts of preterm newborns. Journal of Magnetic Resonance Imaging 22, 467–474.

Pierpaoli, C., Barnett, A., Pajevic, S., Chen, R., Penix, L., Virta, A., Basser, P., 2001. Water diffusion changes in wallerian degeneration and their dependence on white matter architecture. NeuroImage 13, 1174–1185.

Puig, J., Pedraza, S., Blasco, G., Daunis-i-Estadella, J., Prats, A., Prados, F., Boada, I., Castellanos, M., Sánchez-González, J., Remollo, S., Laguillo, G., Quiles, A.M., Gómez, E., Serena, J., 2010. Wallerian degeneration in the corticospinal tract evaluated by diffusion tensor imaging correlates with motor deficit 30 days after middle cerebral artery ischemic stroke. American Journal of Neuroradiology 31, 1324–1330.

Puig, J., Pedraza, S., Blasco, G., Daunis-i-Estadella, J., Prados, F., Remollo, S., Prats-Galino, A., Soria, G., Boada, I., Castellanos, M., Serena, J., 2011. Acute damage to the posterior limb of the internal capsule on diffusion tensor tractography as an early imaging predictor of motor outcome after stroke. American Journal of Neuroradiology 32, 857–863.

Qiu, M., Darling, W.G., Morecraft, R.J., Ni, C.C., Rajendra, J., Butler, A.J., 2011. White matter integrity is a stronger predictor of motor function than BOLD response in patients with stroke. Neurorehabilitation and Neural Repair 25, 275–284.

Riley, J.D., Le, V., Der-Yeghiaian, L., See, J., Newton, J.M., Ward, N.S., Cramer, S.C., 2011. Anatomy of stroke injury predicts gains from therapy. Stroke 42, 421–426.

Ripollés, P., Marco-Pallarés, J., De Diego-Balaguer, R., Miró, J., Falip, M., Juncadella, M., Rubio, F., Rodriguez-Fornells, A., 2012. Analysis of automated methods for spatial normalization of lesioned brains. NeuroImage 60, 1296–1306.

Rüber, T., Schlaug, G., Lindenberg, R., 2012. Compensatory role of the cortico-rubrospinal tract in motor recovery after stroke. Neurology 79, 515–522.

Schulz, R., Park, C.H., Boudrias, M.H., Gerloff, C., Hummel, F.C., Ward, N.S., 2012. Assessing the integrity of corticospinal pathways from primary and secondary cortical motor areas after stroke. Stroke 43, 2248–2251.

Smith, S.M., Jenkinson, M., Johansen-Berg, H., Rueckert, D., Nichols, T.E., Mackay, C.E., Watkins, K.E., Ciccarelli, O., Cader, M.Z., Matthews, P.M., Behrens, T.E.J., 2006. Tract-based spatial statistics: Voxelwise analysis of multi-subject diffusion data. NeuroImage 31, 1487–1505.

Squarcina, L., Bertoldo, A., Ham, T.E., Heckemann, R., Sharp, D.J., 2012. A robust method for investigating thalamic white matter tracts after traumatic brain injury. NeuroImage 63, 779–788.

Stinear, C.M., Barber, P.A., Smale, P.R., Coxon, J.P., Fleming, M.K., Byblow, W.D., 2007. Functional potential in chronic stroke patients depends on corticospinal tract integrity. Brain 130, 170–180.

Stinear, C.M., Barber, P.A., Petoe, M., Anwar, S., Byblow, W.D., 2012. The PREP algorithm predicts potential for upper limb recovery after stroke. Brain 135, 2527–2535.

Sunderland, A., Tinson, D., Bradley, L., Langton Hewer, R., 1989. Arm function after stroke. An evaluation of grip strength as a measure of recovery and a prognostic indicator. Journal of Neurology, Neurosurgery, and Psychiatry 52, 1267–1272.

Tang, P.F., Ko, Y.H., Luo, Z.A., Yeh, F.C., Chen, S.H.A., Tseng, W.Y.I., 2010. Tract-specific and region of interest analysis of corticospinal tract integrity in subcortical ischemic stroke: reliability and correlation with motor function of affected lower extremity. American Journal of Neuroradiology 31, 1023–1030.

Wiegell, M.R., Larsson, H.B., Wedeen, V.J., 2000. Fiber crossing in human brain depicted with diffusion tensor MR imaging. Radiology 217, 897–903.

Yeo, S.S., Ahn, S.H., Choi, B.Y., Chang, C.H., Lee, J., Jang, S.H., 2011. Contribution of the pedunculopontine nucleus on walking in stroke patients. European Neurology 65, 332–337.

Yu, C., Zhu, C., Zhang, Y., Chen, H., Qin, W., Wang, M., Li, K., 2009. A longitudinal diffusion tensor imaging study on Wallerian degeneration of corticospinal tract after motor pathway stroke. NeuroImage 47, 451–458.